Supporting Information for:

Promoting 2D growth in transition metal sulfide semiconductor nanostructures via halide ions

Wen-Ya Wu[1,2,§], Sabyasachi Chakrabortty [1,§], Corina K. L. Chang[1], Asim Guchhait[1], Ming Lin [2]*, and Yinthai Chan[1,2]*

[1]Department of Chemistry, National University of Singapore, 3 Science Drive 3, Singapore 117543 (Singapore)

[2]Institute of Material Research & Engineering, A-STAR, 3 Research Link, Singapore, 117602 (Singapore)

E-mail: chmchany@nus.edu.sg; m-lin@imre.a-star.edu.sg

Homepage: http://staff.science.nus.edu.sg/~chmchany/Home.html

[§]These authors contributed equally to this work.

I Additional characterization data:

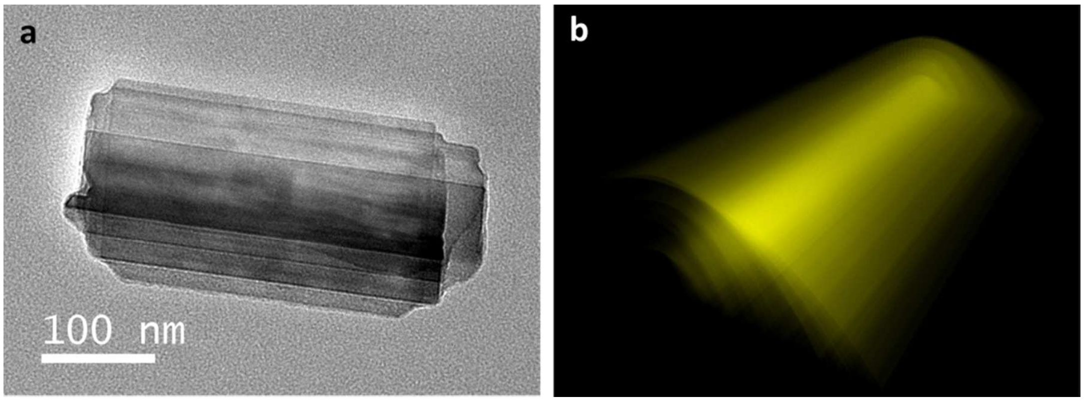

Figure S1. (a) TEM image of multiple sheet-like Ni_9S_8 stacked in parallel. (b) Schematic illustration of Ni_9S_8 sheets within a stack. When incomplete growth of the four wings occurs, Ni_9S_8 nanoplates have a more belt-like morphology and can form a stack comprising of multiple nanosheets.

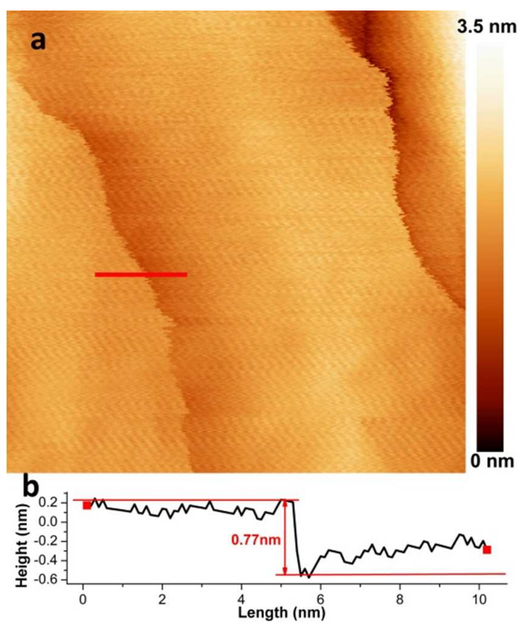

Figure S2. (a) AFM image which shows a series of step-edges on the synthesized Ni_9S_8 nanoplates. (b) Height profile across a typical step-edge, which shows that the average thickness of each step is around ~ 0.8 nm.

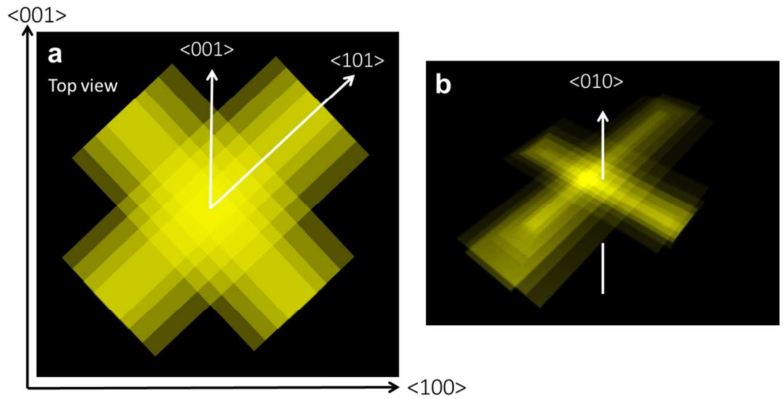

Figure S3. Schematic illustration of growth axes of a cross Ni_9S_8 nanoplate from (a) top-view and (b) 45^o angled side view respectively.

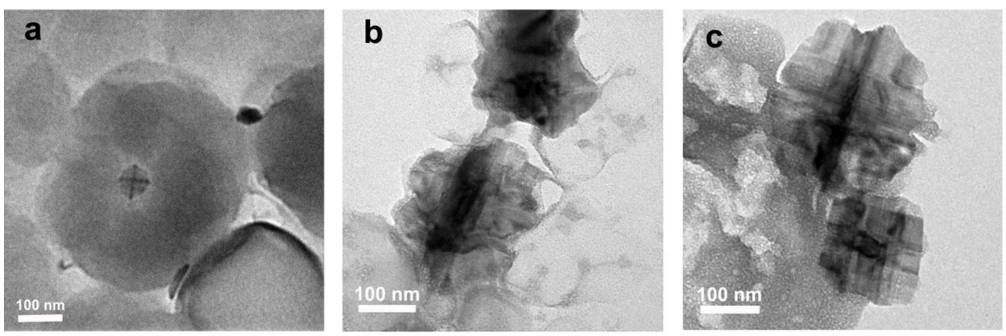

Figure S4. Growth evolution of Ni_9S_8 nanocrystals from (a) 230 ^{o}C, (b) 250 ^{o}C, (c) maintained at 250 ^{o}C for 5 min.

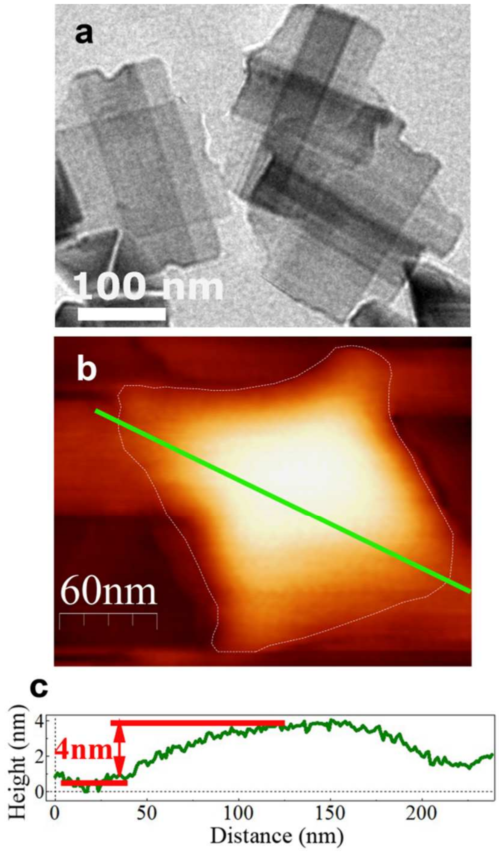

Figure S5. Ni_9S_8 nanoplates obtained at lower Ni(II) precursor concentration. (a) TEM image of the Ni_9S_8 sheet; (b) AFM image of a single Ni_9S_8 sheet; (c) Height profile across the green line in (b) showing that the height is around 4 nm. Given the ligands at the basal planes, the thickness of the sheet is therefore less than 4 nm.

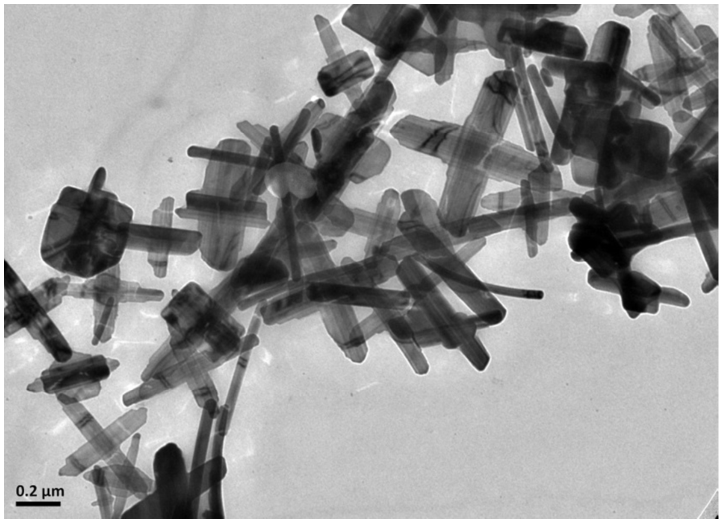

Figure S6. Low resolution TEM image of Ni_9S_8 nanostructures obtained using $NiBr_2$ as the precursor, where all the other parameters were kept the same as that of the synthesis with Cl^-, with the sole exception that the growth temperature was set at 265 - 270 ^oC. The resulting nanocrystals were several times larger in dimensions and with a poorer size distribution compared with those using Cl^-, but clearly exhibited a cross-like plate morphology.

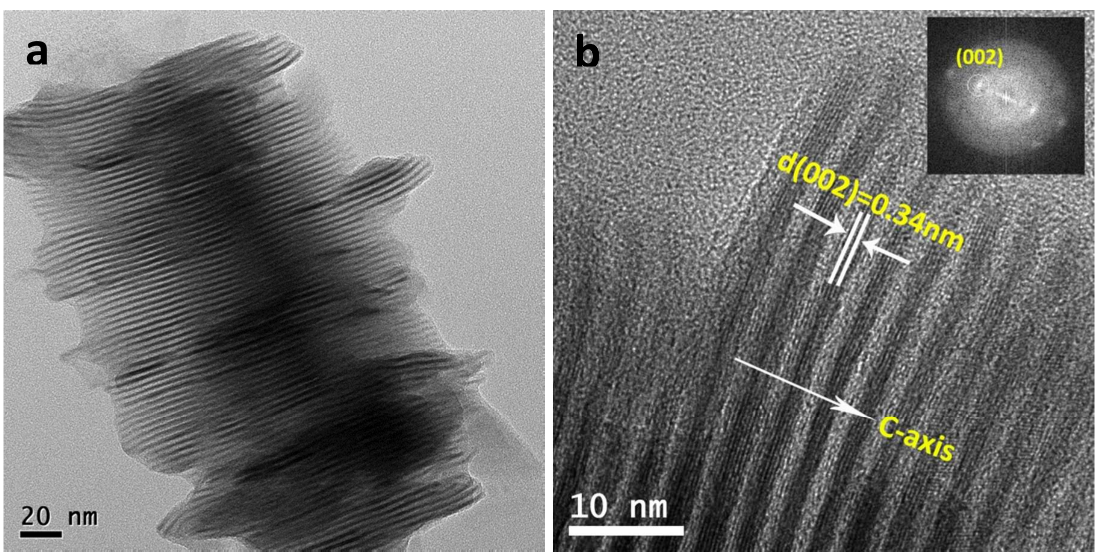

Figure S7. a) TEM image of stacks of ultrathin Cu_2S nanoplates, where the average thickness of these sheets are below 2 nm; b) Corresponding HRTEM image of the same sample, showing a lattice d-spacing of 0.34 nm which represents the (0 0 2) plane. Inset shows the FFT of the selected area where the (0 0 2) plane spot in the pattern is clearly evident.

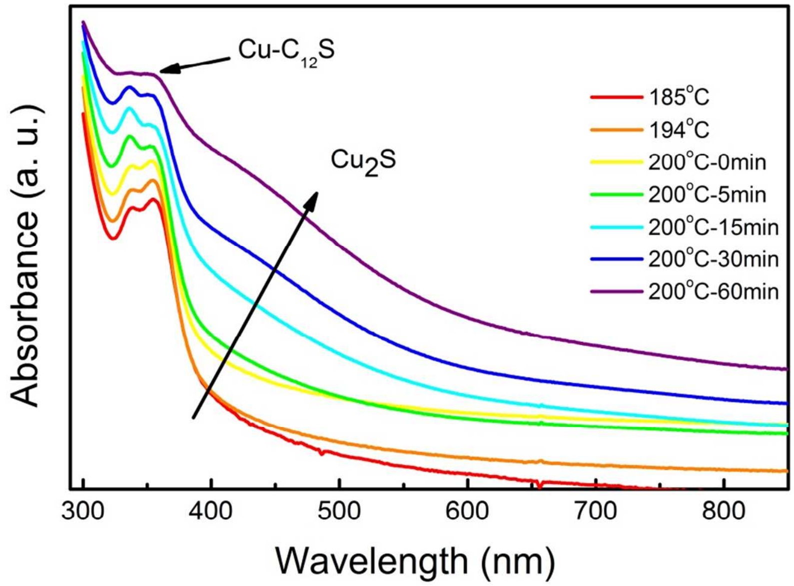

Figure S8. UV-Vis spectra of the aliquots taken from reaction pot during the Cu_2S growth. The absorbance peaks at the lower wavelength range of 330-360 nm is attributed to the Cu-dodecanethiolate bond. These 2 peaks are gradually decreasing due to the breakdown of dodecanethiolate during the growth of the Cu_2S nanocrystal. As the reaction proceeds, the Cu_2S absorbance band (400 ~550 nm) starts to emerge and becomes more prominent as the Cu thiolate peak decreases.

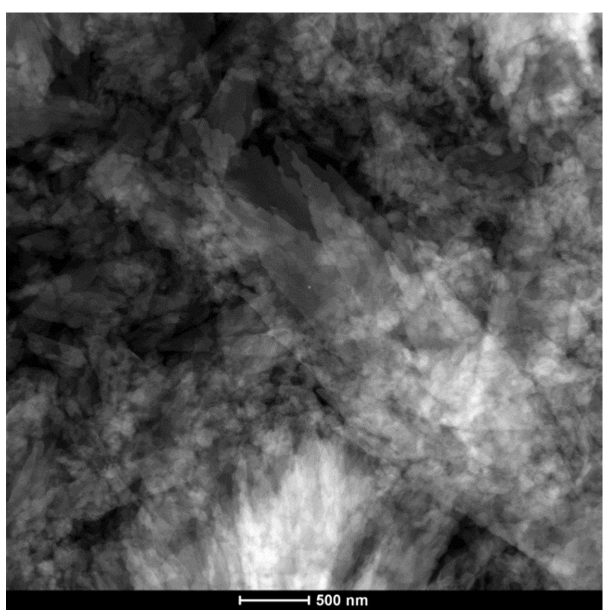

Figure S9. HAADF-STEM image of a preformed film comprising of Cu, S and Cl. Consumption of the film eventually leads to the nucleation and growth of Cu_2S nanoplates.

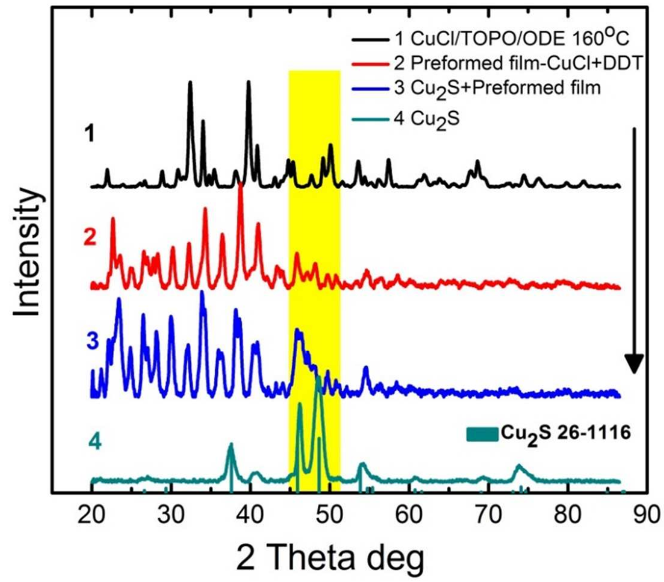

Figure S10. The evolution of XRD from (1) CuCl.H_2O (2) the preformed film after DDT injection to the pot, when the growth temperature was at 200 °C, (3) the Cu_2S nanoplates in co-existence with the preformed film of Cu thiolate, to (4) the final Cu_2S nanoplates. (All samples were prepared in powder form).

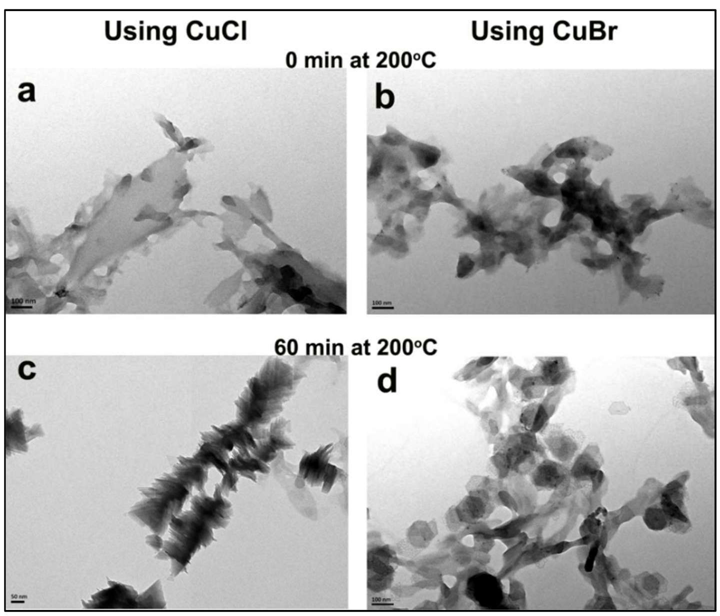

Figure S11. TEM images of experiments comparing the rate of consumption of the preformed film while using (a,c) CuCl and (b,d) CuBr as the Cu precursor respectively. When the reaction temperature reached 200 °C, both aliquots showed a similar looking preformed film structure, however after growth at (c) 200 °C for 60 min, the preformed films were almost fully consumed, leaving a large number of Cu_2S nanoplates; on the other hand, the consumption of the preformed film in the case of CuBr was very slow, and it is seen in (d) that a significant fraction of the preformed film remained even after 60 min of growth. Nevertheless, it is seen that hexagonal-shaped Cu_2S nanosplates were produced.

Table S1. Elemental analysis on preformed film.

Cu	Cu(w%)	S(w%)	Cl(w%)	Br(w%)	Cu:S:Halide(mol)
Preformed film(Cl)	18.86%	11.27%	1.30%		1 : 0.83 : 0.11
Preformed film(Br)	23.79%	9.86%		1.43%	1 : 1.2 : 0.12
Ni	Ni(w%)	S(w%)	Cl(w%)		Ni:S:Halide(mol)
Preformed film(Cl)	24.17%	1.87%	27.17%		1 : 0.14 : 1.8

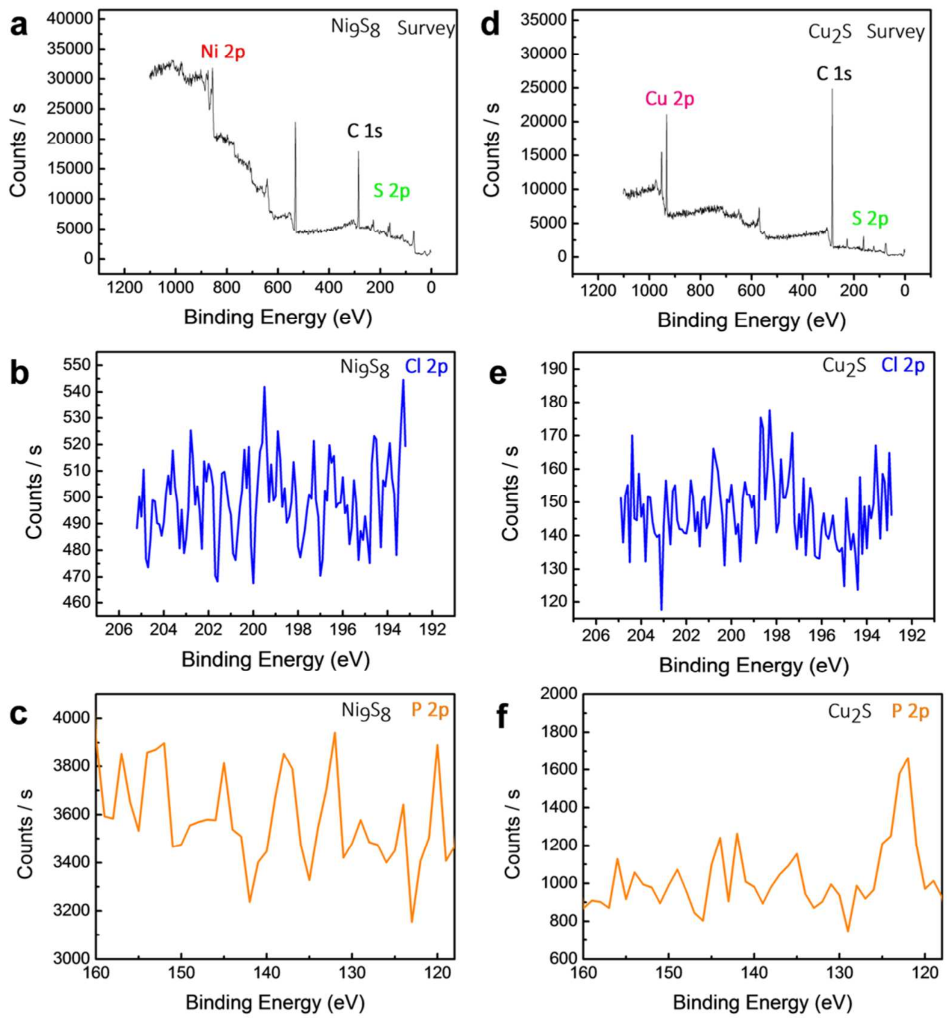

Figure S12. XPS of (a) Ni_9S_8, (d) Cu_2S nanoplates, where Cl 2p signal window is further elaborated in (b) and (e) respectively, (c) and (f) is the signal of P 2p. We did not get any observable Cl and P signal from both of our final nanoplates.